Jahn-Teller effect and Electron Correlation in manganites

Ryo Maezono

Theory of Condensed Matter Group, Cavendish Laboratory, University of Cambridge,

Madingley Road, Cambridge CB3 0HE, U.K.

National Institute for Materials Science, Computational Materials Science Division,

Sengen 1-2-1, Tsukuba, Ibaragi, 305-0047, Japan.

Naoto Nagaosa

Department of Applied Physics, University of Tokyo, Bunkyo-ku, Tokyo 113-8656, Japan.

Correlated Electron Research Center (CERC), National Institute of Advanced Industrial Science

and Technology (AIST), Tsukuba Central 4, Tsukuba 305-8562, Japan.

(February 1, 2008)

Abstract

Jahn-Teller (JT) effect both in the absence and presence of the strong Coulomb correlation is studied theoretically focusing on the reduction ΔK of the kinetic energy gain which is directly related to the spin wave stiffness. Without the Coulomb interaction, the perturbative analysis gives $\Delta K/(g^2/M\Omega^2) \cong 0.05 - 0.13$ depending on the electron number [g: electron-phonon(el-ph) coupling constant, M: mass of the oxygen atom, Ω: frequency of the phonon]. Although there occurs many channels of the JT el-ph interaction in the multiband system, the final results of ΔK roughly scales with the density of states at the Fermi energy. In the limit of strong electron correlation, the magnitude of the orbital polarization saturate and the relevant degrees of freedom are the direction (phase) of it. An effective action is derived for the phase variable including the effect of the JT interaction. In this

limit, JT interaction is *enhanced* compared with the non-interacting case, and ΔK is given by the lattice relaxation energy E_L for the localized electrons, although the electrons remains itinerant. Discussion on experiments are given based on these theoretical results.

71.27.+a, 75.30.-m, 75.30.Et

Typeset using REVTEX

I. INTRODUCTION

It has been recognized that in the strongly correlated electronic systems both the electron-phonon (el-ph) and electron-electron (el-el) interaction are enhanced and play important roles. In manganites, the colossal magneto-resistance (CMR)[1−4] has been discussed from both points of view. In this system the ferromagnetism is basically explained by the double exchange model.[5−7] However the orbital degeneracy of the e_g-states is considered to be very important, and the orbital ordering or disordering is the crucial issue for the understanding of the CMR effect.[8−15] Therefore there are two viewpoints on this problem, namely the orbital degrees of freedom is governed by (i) the Jahn-Teller (JT) electron-phonon coupling or (ii) the electron correlation. In the former case, the change of the bandwidth due to the crossover from small to large JT-polaron is the key mechanism of the CMR effect, and the JT effect is assumed to be negligible in the ferromagnetic metallic state.[16−20] This picture appear contradicting with the orbital orderings, which require rather strong coupling, surrounding the ferromagnetic region in the phase diagram.[11,21−33] However it might be the case that the metallic screening weakens the el-ph interaction and/or the el-el interaction, and only in the ferromagnetic metallic state both of them could be neglected although the Hund's coupling is strong enough to polarize the spins perfectly. On the other hand, it has been recognized by several authors[8−15,27,34] that the Coulomb interaction play the important role in the physics of the orbital degrees of freedom, and the JT-interaction is the secondary effect.

In this paper we revisited this issue by considering both the el-ph and el-el interaction, because both of them are considered to be relevant. Then the interplay between these two interactions is the key issue. As shown below, the metallic screening of the JT el-ph interaction does not occur in contrast to the coupling between the breathing mode and the charge fluctuation. Coulomb interaction and JT effect collaborate with each other, and it is concluded that JT effect is *enhanced* by the el-el interaction by comparing the two limits of zero and strong electron correlations. Similar idea has been proposed by one of

the authors[9] in the context of the large-d approximation[16−20,35], where the single site model embedded in the dymanical environment is considered[36]. To our knowledge the effect of the JT phonon scattering with $d = 3$ has not yet been exploited so much, and we found that the el-ph coupling which modulates the transfer integral becomes relevant in both limits of the non-interacting and the strong correlation limit. Another important issue is how the el-ph intereaction manifests itself in the spin stiffness observed in neutron scattering experiments[37]. Because of the half-metallicity, the stiffness is roughly proportional to the kinetic energy.[38] The polaronic effect on the kinetic energy is therefore expected to appear as a reduction of the stiffness.[37,38]. The apparent absence of this reduction has led to the conclusion that el-ph interaction is irrelevant in the ferromagnetic metallic state. However we found that JT el-ph interaction is there even in the ferromagnetic state although it might be hidden in the inaccuracy of the theoretical estimation of the bare spin stiffness compared with the experimental ones. We expect near 3% of the reduction of the kinetic energy and spin stiffness due to the JT interaction as a lower bound estimated in the non-interacting limit.

We first consider the non-interacting electrons with orbital degeneracy with JT el-ph coupling.[27] The single-band model where the charge density is coupled to the phonon can be treated by means of the canonical transformation, leading to the reduction of the kinetic energy via the Debye-Waller factor.[39] This argument is applicable to the interaction with the breathing mode. However this method can not be generalized to the JT el-ph interaction with multiband electronic structure because it includes off-diagonal components with respect to orbital indices. Due to this difficulty, it is hard to apply the same argument as the breathing mode case to clarify whether the JT polaron also leads to the reduction of the kinetic energy or not. Therefore we employ the perturbative analysis on the JT el-ph coupling to estimate the reduction of the kinetic energy and spin stiffness. Although many channels contribute, each of which can be even negative, the resultant reduction in the kinetic energy gain is roughly proportional to the density of states at the Fermi energy, and has a peak at around $n = 0.6$ and $n = 1.4$, where n denotes the filling of the e_g band.

Next we consider the strong correlation limit by employing the effective Lagrangian which is derived as a projection onto the polarized orbital state.[27] In this limit, the magnitude of the orbital polarization has been saturated, and the only degrees of freedom coupled to the JT phonon is therefore the direction of the polarization (which corresponds to the shape of the orbital ordering). The direction is determined by the double exchange interaction, which is of the order of the transfer integral, t_0. The quantum fluctuation of the direction (physically the fluctuation of the orbital shape) is couples to the lattice deformation via the el-ph interaction, leading to the lattice relaxation energy $E_L = g^2/M\Omega^2$ (g, M and Ω denote the JT el-ph coupling constant, the atomic mass, and the phonon frequency, respectively). The characteristic frequency ω_n of the orbital fluctuation is of the order of the transfer integral t_0, and is larger than the phonon frequency Ω. Namely the orbital deformation can follow up the phonon, leading to the kinetic energy correction, $\Delta K \sim E_L$. The phonon frequency (Ω-) dependence of the kinetic energy correction in this case, $[\Delta K_{U\to\infty}(\Omega)/E_L] \sim O(1)$, is different from that of non-interacting electrons case, $[\Delta K_{U=0}(\Omega)/E_L] \sim \left[(\Omega/t_0)/(1+\Omega/t_0)^2\right]$. Thus the strong correlation enhances the JT effect, in sharp contrast to the case of breathing mode where the Coulomb interaction reduces the el-ph interaction. This is understood rather easily. In the case of the breathing mode, the Coulomb interaction suppresses the charge fluctuation while the breathing mode induces it, i.e., these two interactions compete with each other, and the former suppresses the latter. Furthermore the metallic screening effect also suppresses the charge fluctuation (This situation has been discussed in the context of the vertex correction of the el-ph interaction in the physics of high-T_c cuprates[40]). On the other hand, in the JT mode case, where el-el and el-ph interactions collaborate to induce the orbital pseudospin moment, the former enhances the latter and vice versa. Therefore there is no reason to expect the weakening of the JT el-ph interaction with the doping when the strong el-el interaction keeps the orbital pseudo-spin moment to saturate even in the ferromagneitc metallic state.

The plan of this paper follows. The perturbative analysis of the JT el-ph interaction for the noninteracting electrons with orbital degeneracy is given in Section II. The strong

correlation limit is studied in Sec. III, and discussion and conclusions are presented in Sec. IV.

II. NON-INTERACTING LIMIT

The JT interaction is given as

$$H_{JT} = g \sum_j \left[\left(d_{ja}^\dagger d_{ja} - d_{jb}^\dagger d_{jb} \right) \cdot Q_{u,j} + \left(d_{ja}^\dagger d_{jb} + d_{jb}^\dagger d_{ja} \right) \cdot Q_{v,j} \right] , \tag{1}$$

with a coupling constant g. The spinless operator for the half-metallic ferromagnetic phase, $d_{j\gamma}^\dagger$, creates a spin polarized e_g electron with orbital γ $[= a(d_{x^2-y^2}), b(d_{3z^2-r^2})]$ at site j. Q_u and Q_v denote the normal coordinates of the displacement of the oxygen ions Δ_α ($\alpha = x, y, z$): $Q_u = (2\Delta_z - \Delta_x - \Delta_y)/\sqrt{6}$, $Q_v = (\Delta_x - \Delta_y)/\sqrt{2}$. Let us consider the kinetic energy correction due to the JT phonon scattering with a two-band model,

$$H = \sum_{i\delta,\gamma\gamma'} t_{i,i+\delta}^{\gamma\gamma'} \cdot d_{i\gamma}^\dagger d_{i+\delta,\gamma'} + \sum_j \left[\frac{1}{2M} \vec{P}_j \cdot \vec{P}_j + \frac{M\Omega^2}{2} \vec{Q}_j \cdot \vec{Q}_j \right] + H_{JT} . \tag{2}$$

$\left\{ t_{i,i+\delta}^{\gamma\gamma'} \right\}$ are realistic anisotropic hopping intensities given in ref.[27]. $\vec{Q}_j$ is defined as $(Q_{u,j}, Q_{v,j})^t$. M, Ω, and $\vec{P}_j$ denote the atomic mass, the elastic constant, and the canonical momentum of $\vec{Q}_j$, respectively. For a simplified model without orbital indices, the canonical transformation is a standard method to deal with the electron-phonon interaction, leading to the kinetic energy reduction by the Debye-Waller factor.[39] The canonical transformation for the JT phonon has off-diagonal elements with respect to orbital indices, due to which the application of this method becomes complicated. We therefore employ the perturbative calculation of the kinetic energy K up to the second order with respect to the coupling constant g, as

$$K = K_0 + \Delta K , \ \Delta K \sim O\left(g^2\right) . \tag{3}$$

ΔK is expressed by diagrams of the self-energy shown in Fig. 1.
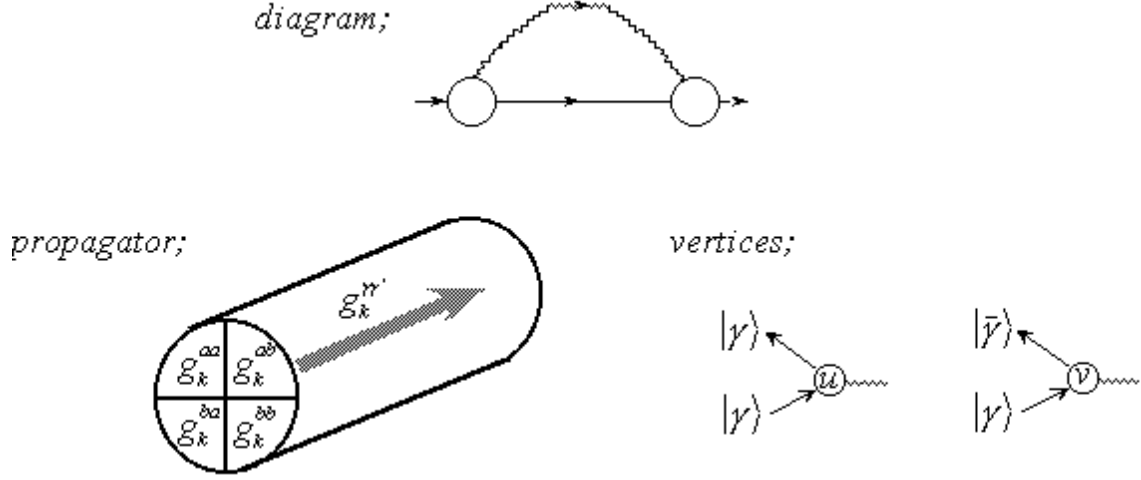
diagram;

propagator;　　　　　　　　　　　　　　　　*vertices;*

FIG. 1. Diagrams of the self-energy due to the JT interaction. Correponding to the doubly degenerate orbitals, there are two kinds of vertices and the diagram is composed with four-channeled propagator.

There are two vertices corresponding to Q_u- and Q_v-scatterings. The propagator takes 2×2-matrix form with respect to the orbital indices. Annihilation and creation operators of the JT phonons are introduced as

$$Q_{u,v}(t) = \sqrt{\frac{1}{2M\Omega}} \cdot \left(a_{u,v} \cdot e^{-i\Omega t} + a_{u,v}^\dagger \cdot e^{i\Omega t} \right) . \tag{4}$$

With the momentum representation of the operators $c = (a, d)$,

$$c_j(\tau) = \frac{1}{\sqrt{\beta N}} \sum_{j,l} c_q(i\omega_l) \cdot e^{iqR_j - i\omega_l \tau} \quad , \quad i\omega_l \to z , \tag{5}$$

with Matsubara frequency $i\omega_l$, the propagators of electrons and phonons are given as

$$g_k^{\gamma\gamma'}(z) = -T \left\langle d_{k\gamma}(z) d_{k\gamma'}^\dagger(z) \right\rangle_{0;i\omega_l=z} = \left[(z+\mu)\delta_{\gamma\gamma'} - \varepsilon_k^{\gamma\gamma'} \right]_{\gamma\gamma'}^{-1} = \frac{A_{+;k}^{\gamma\gamma'}}{z - \Xi_k^{(+)}} + \frac{A_{-;k}^{\gamma\gamma'}}{z - \Xi_k^{(-)}} , \tag{6}$$

$$\begin{aligned} D_q^{u(v)}(z) &= \frac{1}{2NM\Omega} \cdot \left[T \left\langle a_{q,u(v)}(z) a_{q,u(v)}^\dagger(z) \right\rangle + T \left\langle a_{-q,u(v)}^\dagger(z) a_{-q,u(v)}(z) \right\rangle \right] \\ &= \frac{1}{2NM\Omega} \cdot \left[\frac{1}{z+\Omega} - \frac{1}{z-\Omega} \right] = D_q(z) , \end{aligned} \tag{7}$$

respectively. The u- and v-modes have the same mass and frequency because they belong to the same irreducible representation, and then the same phonon propagator. Here we

neglected the inter-cluster coupling of the vibration and hence the wavelength dependence of the phonon frequency. Coefficients $A_{\pm;k}^{\gamma\gamma'}$ in Eq. (6) are defined as

$$A_{+;k}^{\gamma\gamma} = \frac{\Xi_k^{(+)} - \xi_k^{\bar\gamma}}{\Xi_k^{(+)} - \Xi_k^{(-)}} \quad , \quad A_{-;k}^{\gamma\gamma} = -\frac{\Xi_k^{(-)} - \xi_k^{\bar\gamma}}{\Xi_k^{(+)} - \Xi_k^{(-)}} ,$$

$$A_{+;k}^{\gamma\bar\gamma} = \frac{-\varepsilon_k^{ab}}{\Xi_k^{(+)} - \Xi_k^{(-)}} \quad , \quad A_{-;k}^{\gamma\bar\gamma} = -\frac{-\varepsilon_k^{ab}}{\Xi_k^{(+)} - \Xi_k^{(-)}} , \tag{8}$$

with dispersion relations of the hybridized bands given as

$$\Xi_k^{(\pm)} = \frac{1}{2}\left[\left(\xi_k^a + \xi_k^b\right) \pm \sqrt{\left(\xi_k^a - \xi_k^b\right)^2 + 4\left(\varepsilon_k^{ab}\right)^2}\right] \quad , \quad \xi_k^\gamma = \varepsilon_k^\gamma - \mu . \tag{9}$$

The orbital index $\bar\gamma$ is used as $\bar a = b$ and $\bar b = a$. $\varepsilon_k^{aa}\,(=\varepsilon_k^a)$, $\varepsilon_k^{bb}\left(=\varepsilon_k^b\right)$, and ε_k^{ab} are the cosine dispersions with overlap integrals between the orbitals $|a\rangle = |x^2 - y^2\rangle$ and $|b\rangle = |3z^2 - r^2\rangle$. With the propagators, the kinetic energy correction ΔK is given as

$$\Delta K = \frac{1}{2}\sum_l \sum_{k,\gamma\gamma'} \sum_{\gamma_1\gamma_2} \varepsilon_k^{\gamma\gamma'} g_{\vec k}^{\gamma\gamma_1}(i\omega_l) \cdot \Sigma_{\vec k}^{\gamma_1\gamma_2}(i\omega_l) \cdot g_{\vec k}^{\gamma_2\gamma'}(i\omega_l) , \tag{10}$$

$$\Sigma_{\vec k}^{\gamma_1\gamma_2}(i\omega_l) = -\frac{g^2}{\beta}\sum_q \oint_c \frac{dz}{2\pi i}\cdot f(z)\left[g_{\vec k-\vec q}^{\gamma_1\gamma_2}(z) + g_{\vec k-\vec q}^{\bar\gamma_1\bar\gamma_2}(z)\right]\cdot D_q(i\omega_l - z) , \tag{11}$$

where the contour c surrounds the poles of the fermi distribution function $f(z)$. In Eq. (11), $g_{\vec k-\vec q}^{\gamma_1\gamma_2}(z)$ and $g_{\vec k-\vec q}^{\bar\gamma_1\bar\gamma_2}(z)$ correspond to the scattering by u- and v-vertex, respectively. These contributions are represented by diagrams shown in Fig. 2.
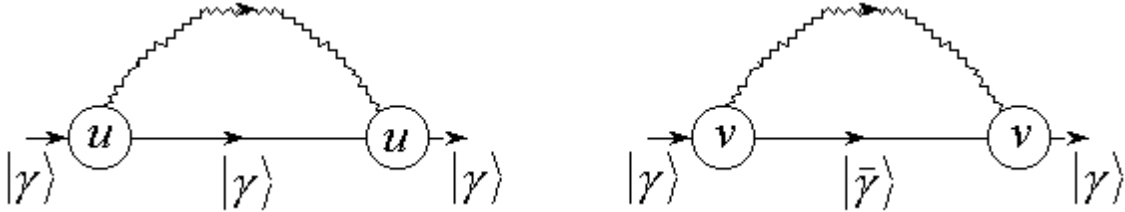

FIG. 2. Corresponding diagrams of the terms in Eq. (11).

Introducing a notation,

$$I_{(\gamma_2\gamma_2';\gamma_3\gamma_3')}^{(\gamma_1\gamma_1')}(k) = \sum_l \Sigma_{\vec k}^{\gamma_1\gamma_1'}(i\omega_l) \cdot g_{\vec k}^{\gamma_2\gamma_2'}(i\omega_l) g_{\vec k}^{\gamma_3\gamma_3'}(i\omega_l) , \tag{12}$$

Eq. (10) is expanded as,

8

$$\Delta K = \frac{1}{2} \sum_k \left[\varepsilon_k^{aa} \cdot I_{(aa;aa)}^{(aa)} + \varepsilon_k^{aa} \cdot I_{(ab;ab)}^{(aa)} + 2\varepsilon_k^{ab} \cdot I_{(ab;aa)}^{(aa)} \right]$$

$$+ \frac{1}{2} \sum_k \left[\varepsilon_k^{bb} \cdot I_{(bb;bb)}^{(bb)} + \varepsilon_k^{bb} \cdot I_{(ab;ab)}^{(bb)} + 2\varepsilon_k^{ab} \cdot I_{(ab;bb)}^{(aa)} \right]$$

$$+ \sum_k \left[\varepsilon_k^{aa} \cdot I_{(ab;aa)}^{(ab)} + \varepsilon_k^{bb} \cdot I_{(ab;bb)}^{(ab)} + \varepsilon_k^{ab} \cdot \left(I_{(ab;ab)}^{(ab)} + I_{(aa;bb)}^{(ab)} \right) \right] . \qquad (13)$$

Three terms correspond to the contribution from Σ_k^{aa}, $\Sigma_k^{bb} (= \Sigma_k^{aa})$, and Σ_k^{ab}, respectively. Note that the upper (lower) suffix $\gamma_n \gamma_n'$ of $I_{(\gamma_2 \gamma_2'; \gamma_3 \gamma_3')}^{(\gamma_1 \gamma_1')}$ means that the correpsonding contribution comes from a diagram composed of a propagator $g_{k-q}^{\gamma_n \gamma_n'}$ $\left(g_k^{\gamma_n \gamma_n'} \right)$ for the state $|k - q\rangle$ $(|k\rangle)$ [When one finds (ab) in the upper (lower) suffix, that contribution contains the hybridization during the propagation with the wave vector $|k - q\rangle$ $(|k\rangle)$]. In Appendix A are given concrete forms of $I_{(\gamma_2 \gamma_2'; \gamma_3 \gamma_3')}^{(\gamma_1 \gamma_1')}$.

Numerical results are shown in Fig. 3 with parameters $t_0 = 0.72$ eV[27] and $\Omega = 0.05$ eV.[45] The kinetic reduction ΔK is calculated as a function of the filling n.
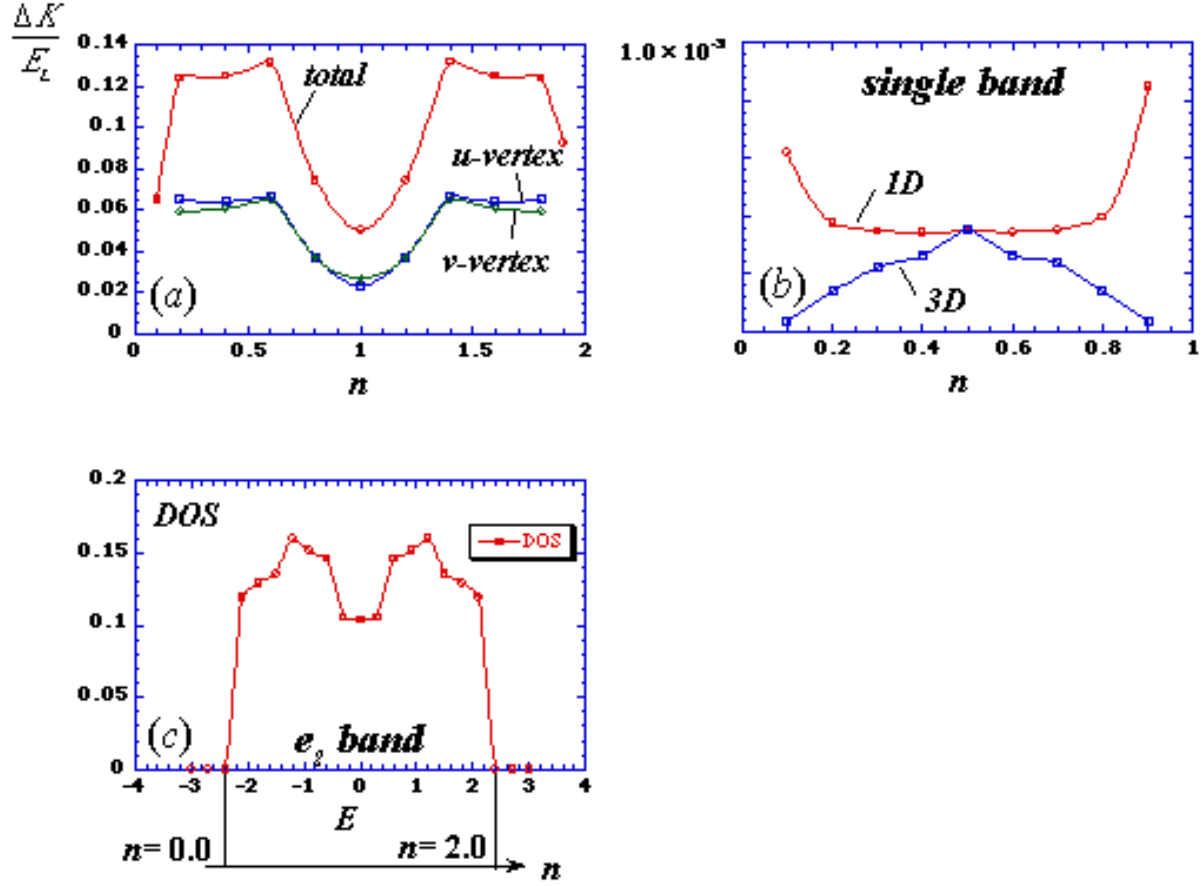
FIG. 3. Kinetic energy reduction as a function of the filling n for non-interacting electrons. (a) Total result and partial contributions from u- and v-vertices in a realistic two-band model with e_g anisotropy. (b) Result for one and three dimensional single band cases with breathing type phonons. (c) Density of states as a function of the fermi energy for given n (lower n-axis) in the system used for (a).

Panel (a) shows the total result [Eq. (13)] and partial contributions due to the u- and v-vertices. The particle-hole symmetry with respect to the axis $n = 1.0$ is seen. The positive definite result is obtained for the whole range of n. In order to understand the origin of the n-dependence in the plot (a), we also calculate the simpler case with breathing type phonons and single band electrons [Eq. (A8)] in one and three dimensions, as shown in the panel (b). In this case $\Delta K/E_L$ roughly scales to the density of states at the fermi level $N(\varepsilon_F)$ for given n (see Appendix B). According with this expectation, the result has the minimum

10

(maximum) at $n = 0.5$ for one (three) dimensional case. The positive definite result in the plot (b) is consistent with the consequence from the canonical transformation method.[39] Though the expression for the realistic doubly-degenerate e_g case [Eq. (13) and the panel (a)] is much more complicated, the result also seems to scale to the density of states. For the comparison, the plot of the density of states in this case is shown in the panel (c). Values of n giving the peak and the dip in panel (a) and (c) actually coincide each other. As discussed in Appendix B, k- (wave vector) points near the Fermi level contribute dominantly to ΔK. Unless the n-dependence of each contributing value is so sensitive, ΔK simply scales to the population of the contributing k-points and hence $N(\varepsilon_F(n))$ for given n. This gives a rough explanation for the correlation between $\Delta K(n)$ and $N(\varepsilon_F)$. More intuitively, ΔK scales to the population of electrons around the fermi surface $[\propto N(\varepsilon_F)]$ which is subject to the phonon scattering.

In order to see how each scattering process contributes, we re-divide ΔK into several contributions as

$$
\begin{aligned}
\Delta K = \frac{1}{2} \sum_k \left[\varepsilon_k^{aa} \cdot I_{(aa;aa)}^{(aa)} + \varepsilon_k^{bb} \cdot I_{(bb;bb)}^{(bb)} \right] + \frac{1}{2} \sum_k \left[\varepsilon_k^{aa} \cdot I_{(ab;ab)}^{(aa)} + \varepsilon_k^{bb} \cdot I_{(ab;ab)}^{(bb)} \right] \\
+ \sum_k \left[\varepsilon_k^{ab} \cdot \left(I_{(ab;aa)}^{(aa)} + I_{(ab;bb)}^{(aa)} \right) \right] + \sum_k \left[\varepsilon_k^{aa} \cdot I_{(ab;aa)}^{(ab)} + \varepsilon_k^{bb} \cdot I_{(ab;bb)}^{(ab)} \right] \\
+ \sum_k \left[\varepsilon_k^{ab} \cdot \left(I_{(ab;ab)}^{(ab)} + I_{(aa;bb)}^{(ab)} \right) \right] ,
\end{aligned}
\tag{14}
$$

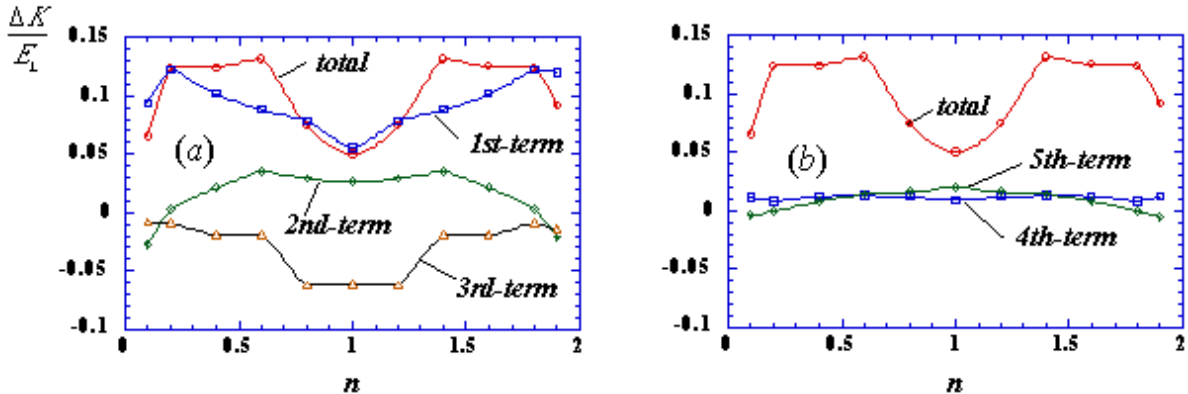and plotted each contribution separately in Fig. 4.

11

The first, second and third terms are coming from $\Sigma_k^{\gamma\gamma}$, whereas the fourth and fifth from $\Sigma_k^{\gamma\bar{\gamma}}$. The latter contribution is small compared with the former. The first term, which is diagonal with respect to the suffices of I, just corresponds to the superposition of two breathing type diagrams with u- and v-vertices, respectively. (Remember the suffix rule of $I_{(\gamma_2\gamma_2';\gamma_3\gamma_3')}^{(\gamma_1\gamma_1')}$ mentioned before). The other terms arise due to the multiband structure and the JT interaction, which are sorted further into two classes. One class (the second and fourth terms) corresponds to the twice inversion of the orbital state (correspondingly the off-diagonal orbital suffix ab appears twice) to come back to the original orbital state (like $a \to b \to a$). Consequently this class picks up the diagonal dispersion $\varepsilon_k^{\gamma\gamma}$ as its weight. The other class (the third and the fifth terms) with odd number the orbital index ab thus picks up the off-diagonal weight ε_k^{ab} (like $a \to a \to b$). Because ε_k^{ab} roughly corresponds to the energy scale of the stabilization due to the band hybridization, it gives basically the negative contribution (stabilization of the energy) as shown by the behavior of the third term in Fig. 4. This stabilization around $n = 1$ is mainly attributed to the dip with negative values of the "3rd-term" seen in Fig. 4 (a). This behavior is understood as follows. The third term $\propto \varepsilon_k^{ab}$ reflects the stabilization of the lower band due to the repulsion with the upper band (its magnitude is $t_{i,i+\delta}^{ab}$). Such a stabilization is most remarkable at the region where the hybridizing two bands cross with each other. For the half-filled case, $n = 1$, the fermi level is located at the middle of the bandwidth, where the band-crossing occurs, leading to the most effective stabilization. That is why the stabilization of the third term is most remarkable around $n = 1$.

III. STRONG CORRELATION LIMIT

Strong on-site repulsions in e_g orbitals can be written as[27]

$$H_{\text{on-site}} = -\tilde{\beta} \sum_j \vec{T}_j \cdot \vec{T}_j \quad , \quad \vec{T}_j = \frac{1}{2} \sum_{\gamma\gamma'} d_{j\gamma}^\dagger \vec{\sigma}_{\gamma\gamma'} d_{j\gamma'} \quad , \tag{15}$$

with spinless operators. $\vec{T}_j$ is the isospin operator representing the orbital degrees of freedom with 2×2 Pauli matrices $\vec{\sigma}_{\gamma\gamma'} = \left(\sigma_{\gamma\gamma'}^x, \sigma_{\gamma\gamma'}^y, \sigma_{\gamma\gamma'}^z\right)$. $\tilde{\beta}$ is a parameter of the electron-electron interaction of the order of the Hubbard repulsive U. This interaction induces the finite orbital polarization, which can be represented by the Stratonovich-Hubbard field (orbital fluctuation field) $\vec{\varphi}_T$ as[27]

$$H_{el} = \sum_{j,\gamma} d_{j\gamma}^\dagger \left(\partial_\tau - \mu\right) d_{j\gamma} + \sum_{i\delta,\gamma\gamma'} t_{i,i+\delta}^{\gamma\gamma'} d_{i\gamma}^\dagger d_{i+\delta,\gamma'} + \sum_j \left[\frac{1}{2M} \vec{P}_j \cdot \vec{P}_j + \frac{M\Omega^2}{2} \vec{Q}_j \cdot \vec{Q}_j + \tilde{\beta}\vec{\varphi}_T^2 \right]$$
$$- \sum_j \vec{T}_j \cdot \left(2\tilde{\beta}\vec{\varphi}_T - g\vec{Q}_j\right) . \tag{16}$$

It is seem that the orbital fluctuation field $\vec{\varphi}_T$ as well as the JT phonon $\vec{Q}$ is coupled to the isospin $\vec{T}$ in the form of linear combination $2\tilde{\beta}\vec{\psi} = 2\tilde{\beta}\vec{\varphi}_T - g\vec{Q}_j$[9]. After integrating out phonon coordinates, the effective action in terms of the field ψ is obtained as

$$S_{\text{eff}} = \int_0^\beta d\tau \left[\sum_{j,\gamma} d_{j\gamma}^\dagger \left(\partial_\tau - \mu\right) d_{j\gamma} + \sum_{i\delta,\gamma\gamma'} t_{i,i+\delta}^{\gamma\gamma'} d_{i\gamma}^\dagger d_{i+\delta,\gamma'} \right] + \tilde{\beta} \sum_{j,n} \frac{2\tilde{\beta}M\left(\omega_n^2 + \Omega^2\right)}{2\tilde{\beta}M\left(\omega_n^2 + \Omega^2\right) + g^2} \cdot \vec{\psi}_{j,n}^* \vec{\psi}_{j,n}$$
$$- 2\tilde{\beta} \sum_{j,n} \vec{T}_{j,n} \cdot \vec{\psi}_{j,n} . \tag{17}$$

where $\omega_n = 2\pi n/\beta$ is the Matsubara frequency for the bosons. The phonon dynamics induces the retardation effect for the field ψ, which is represented by the ω_n-dependence of the second term in the above equation. Now let us assume that the electron correlation is much larger than the JT coupling, namely $\tilde{\beta} \gg E_L$. It is noted here that we do not assume $E_L \ll t_0$, namely the weak coupling limit. Then we can expand in the JT coupling g in eq.(17) as

$$S_{\text{eff}} = \int d\tau \left[\sum_{j,\gamma} d_{j\gamma}^\dagger \left(\partial_\tau - \mu\right) d_{j\gamma} + \sum_{i\delta,\gamma\gamma'} t_{i,i+\delta}^{\gamma\gamma'} d_{i\gamma}^\dagger d_{i+\delta,\gamma'} \right]$$
$$+ \tilde{\beta} \sum_{j,n} \left[1 - \frac{g^2}{2\tilde{\beta}M\left(\omega_n^2 + \Omega^2\right)} \right] \cdot \vec{\psi}_{j,n}^* \vec{\psi}_{j,n} - 2\tilde{\beta} \sum_{j,n} \vec{T}_{j,n} \cdot \vec{\psi}_{j,n} . \tag{18}$$

Because we are now interested in the strong correlation limit, $\tilde{\beta} \gg t_0$, the magnitude of the orbital polarization is fully developed. This corresponds to the fixed $|\vec{\psi}| = \varphi_T = 1/2$, and we consider its direction only within the xz-plane because the JT coupling prefers the real orbital states[27]. Then $\vec{\psi}$ is parametrized as

$$\vec{\psi}_j = \psi \cdot {}^t(\sin\theta_j, 0, \cos\theta_j) \ , \tag{19}$$

with the phase angle θ_j being the only relevant degrees of freedom. Correspondingly, the isospin is forced to be parallel to $\vec{\psi}$, and hence the Grassman variables $d_{j\gamma}^\dagger, d_{j\gamma}$ are replaced by

$$d_{j\gamma} = [f_j \cos(\theta_j/2), f_j \sin(\theta_j/2)]$$
$$d_{j\gamma}^\dagger = {}^t[f_j^\dagger \cos(\theta_j/2), f_j^\dagger \sin(\theta_j/2)] \ , \tag{20}$$

with the spin/orbital-less fermion variable $f^\dagger, f$. Putting this expression into Eq. (18), the kinetic energy term can be written as

$$\sum_{i,\delta} t_{i,i+\delta}(\theta_i, \theta_{i+\delta}) \cdot f_i^\dagger f_{i+\delta} \ , \tag{21}$$

with the θ-dependent transfer integral,

$$t_{i,i+\delta}(\theta_i, \theta_{i+\delta}) = t_{i,i+\delta}^{11} \cos(\theta_i/2) \cos(\theta_{i+\delta}/2) + t_{i,i+\delta}^{22} \sin(\theta_i/2) \sin(\theta_{i+\delta}/2)$$
$$+ t_{i,i+\delta}^{12} \cos(\theta_i/2) \sin(\theta_{i+\delta}/2) + t_{i,i+\delta}^{21} \sin(\theta_i/2) \cos(\theta_{i+\delta}/2) \ . \tag{22}$$

This gives the coupling of θ-field to the fermion. On the other hand, the dynamics of the θ-field is generated through this coupling by integrating over the fermions $f^\dagger, f$.

$$S_{\text{eff}}^0 = \sum_{q,\omega_n} \Pi(\vec{q}, \omega_n) \cdot \theta(\vec{q}, \omega_n)\theta(-\vec{q}, -\omega_n) \ , \tag{23}$$

where θ is measured from the mean field value, and $\Pi(\vec{q}, \omega_n)$ is the orbital correlation function of the fermions. Although the quantitative results depend on the details of the model and the orbital ordering to start with, the orbital fluctuation has a gap of the order of t_0 and there occurs no infrared divergence. Therefore the characteristic frequency ω_n and wavevector $\vec{q}$ for $\Pi(\vec{q}, \omega_n)$ are $\sim t_0$, and π/a (a: lattice constant), respectively. The Hamiltonian consists only of the kinetic energy besides the JT coupling term, and its expectation value is given by

$$\langle H_0 \rangle = \sum_{i,\delta} t_{i,i+\delta}(\theta_i = 0, \theta_{i+\delta} = 0) \left\langle f_i^\dagger f_{i+\delta} \right\rangle_{\text{mean field}} + \lim_{\beta\to\infty} \frac{1}{2\beta} \sum_{\vec{q},\omega} \ln \Pi(\vec{q}, \omega) \ . \tag{24}$$

Now let us analyse the correction term due to the JT interaction

$$\delta S_{\text{eff}} = -\sum_{j,n} \frac{g^2}{2M\left(\omega_n^2 + \Omega^2\right)} \cdot \vec{\psi}_{j,n}^* \vec{\psi}_{j,n} = \sum_{j,n} A\left(i\omega_n\right) \cdot \vec{\psi}_{j,n}^* \vec{\psi}_{j,n} \ . \tag{25}$$

The differential operator $A\left(i\omega_n\right)$ on $\vec{\psi}_{j,n}$ leads to the dynamics of the phase angle $\partial_\tau \theta_j$ through the component,

$$\left(\partial_\tau \vec{\psi}_j\right)^* \cdot \left(\partial_\tau \vec{\psi}_j\right) = \psi_j^2 \cdot \left(\partial_\tau \theta_j\right)^2 \ . \tag{26}$$

Hence the contribution to the dynamics of θ-field due to JT coupling is given by

$$\delta S_{\text{eff}} = \sum_{j,n} A\left(i\omega_n\right) \cdot \vec{\psi}_{j,n}^* \vec{\psi}_{j,n} \rightarrow \psi^2 \cdot \sum_{j,n} \left[A\left(i\omega_n\right) - A\left(0\right)\right] \cdot \theta_{j,n} \theta_{j,-n} \ . \tag{27}$$

Now the dymanics of the orbital is determined by the propagator $D(\vec{q}, \omega_n)$ defined by

$$[D(\vec{q}, \omega_n)]^{-1} = \Pi(\vec{q}, \omega_n) + \frac{\psi^2}{2} \cdot E_L \frac{\omega_n^2}{\omega_n^2 + \Omega^2}. \tag{28}$$

There are two limits of interest. In the case of weak coupling, i.e., $E_L \ll t_0$, the dynamics of the orbital is determined by $\Pi(\vec{q}, \omega_n)$ and the characteristic energy is of the order of t_0. Therefore we can replace ω_n in Eq. (28) by $\sim t_0 \gg \Omega$, and the correction of the propagator is of the order of E_L/t_0^2. More explicitly the reduction of the kinetic energy gain ΔK due to JT coupling is estimated by replacing $\ln \Pi$ in Eq. (24) by $-\ln D$ in Eq. (28) as

$$\Delta K \sim \int d\omega \cdot \frac{E_L \omega^2/(\omega^2 + \Omega^2)}{\Pi(\vec{q}, \omega)} \sim E_L \omega_c^2/(\omega_c^2 + \Omega^2) \ , \tag{29}$$

where ω_c is the characteristic frequency of the orbital fluctuation and $\omega_c \sim t_0$. This energy correction quadratically grows up with increasing $\omega_c/\Omega \ll 1$ and then saturates into the lattice relaxation energy $E_L = g^2/M\Omega^2$ with $\omega_c/\Omega \gg 1$. Considering that $\omega_c \sim t_0 \gg \Omega$, we conclude that $\Delta K \sim E_L$. As increasing $E_L(\sim t_0)$, we expect the saturation effect as $\Delta K \sim E_L t_0/(t_0 + E_L)$ as is evident from eq.(28).

The strong couling limit, i.e., $E_L \gg t_0$, is more interesting. In this case, the orbital dynamics is determined by both Π and E_L terms in Eq. (28). More explicitly the propagator is approximated as

$$[D(\vec{q}, \omega_n)]^{-1} \cong t_0 + \frac{\psi^2}{2} \cdot E_L \frac{\omega_n^2}{\omega_n^2 + \Omega^2}, \tag{30}$$

and its characteristic energy scale is then given by

$$\omega_c \cong \Omega \sqrt{\frac{t_0}{E_L}} \ll \Omega. \tag{31}$$

Therefore there occurs the slow down of the orbital motion in this strong coupling limit. However the small polaron effect should be relevant in this case, which can not be treated in the present formalism, and the detailed study on this strong coupling case is left for future studies.

IV. DISCUSSIONS

We now compare the results for the non-interacting and strongly interacting limits. The order estimation of $\Delta K_{U=0}$ for the non-interacting limit is as follows. Rather complicated form of the non-interacting result, Eq. (13), Eq. (A3), Eq. (A6), and Eq. (A7), roughly takes the Ω-dependence as

$$\Delta K_{U=0} \sim t_0 \cdot \left(\frac{g}{\sqrt{M\Omega}} \right)^2 \cdot \frac{1}{(t_0 + \Omega)^2} \cdot = t_0 \cdot \frac{g^2}{M\Omega} \cdot \frac{1}{(t_0 + \Omega)^2} = E_L \cdot \frac{\Omega/t_0}{(1 + \Omega/t_0)^2} \tag{32}$$

The dependence is hence a kind of perturbative forms with the intermediate energy denominator $1/(t_0 + \Omega)^2$ and the vertex $g/\sqrt{M\Omega}$. The small factor Ω/t_0 comes from the fact that only the states with the energy window $\sim \Omega$ near the Fermi energy is influenced by the el-ph interaction. More explicitly,

$$\frac{\Delta K}{K_0} = \frac{\Delta K/E_L}{K_0/E_L} = \frac{(\text{value picked up from Fig.4})}{K_0/E_L}. \tag{33}$$

E_L can be evaluated as ~ 0.6 eV from the literature[19]. With $K_0 \sim 2.16$ eV in our caluculation, and the value ~ 0.1 in Fig. 4, we get $\Delta K/K_0 \sim 3\%$ as a lower bound.

On the other hand, in the strong correlation limit, the effect of Fermi degeneracy and the small factor Ω/t_0 are missing and $\Delta K \sim E_L$. This means that the strong correlation enhances the JT effect. It is reported that the observed spin stiffness is well reproduced

even semiquantitatively by meanfield estimations without considering the el-ph interaction discussed here.[37,38] This means that the small polaronic effect is absent in the metallic region, namely E_L is of the order or less than t_0 (Here t_0 should be interpreted as the "bandwidth" rather than the transfer integral). It is reasonable with the above estimation that $E_L \sim 0.6$ eV.

In summary, we have studied JT el-ph effect in three dimension with and without the electron correlations. In the non-interacting limit, the reduction is calculated as a function of the doping concentration. In this case, the doping dependence is mainly dominated by the density of states at the Fermi energy. It is shown that the kinetic energy is always reduced by the JT el-ph interaction even if the off-diagonal processes in orbital indices are taken into account. The reduction ΔK of the kinetic energy K is estimated as $\Delta K / K \cong 3\%$ in this non-interacting case. This small value is due to the small factor Ω/t_0 occuring in the Fermi degenerate case. In the strong correlation limit, we have derived an effective action to study the el-ph interaction. The small factor Ω/t_0 is missing in this case and el-ph interaction is enhanced by the strong correlation. $\Delta K \sim E_L t_0 / (E_L + t_0)$ is this case without the small polaron formation. From the comparison with experiments and the above results, the small polaron formation is unlikely in the metallic state.

APPENDIX A: EVALUATION OF EQ. (12)

With $\sigma_k \left(z, \xi_{k-q} \right)$ defined by the breathing type self-energy expression[39] as,

$$\Sigma_{\vec{k}}^0 (z) = \frac{g^2}{2N\beta M\omega} \sum_q \left[\frac{f\left(\xi_{k-q}\right) + N\left(\omega\right)}{z - \xi_{k-q}^{-\omega}} - \frac{f\left(\xi_{k-q}\right) + N\left(-\omega\right)}{z - \xi_{k-q}^{+\omega}} \right] \equiv \sum_q \sigma_k \left(z, \xi_{k-q} \right), \quad (A1)$$

the JT type self-energy Eq. (11) can be written as

17

$$\Sigma_{\vec{k}}^{\gamma\gamma'}(z) = \sum_q \left[\left(A_{+;k-q}^{\gamma\gamma'} + A_{+;k-q}^{\bar{\gamma}\bar{\gamma}'} \right) \cdot \sigma_k \left(z, \Xi_{k-q}^{(+)} \right) + \left(A_{-;k-q}^{\gamma\gamma'} + A_{-;k-q}^{\bar{\gamma}\bar{\gamma}'} \right) \cdot \sigma_k \left(z, \Xi_{k-q}^{(-)} \right) \right] , \quad \text{(A2)}$$

with coefficients $A_{\pm;k}^{\gamma\gamma'}$ defined in Eq. (8). $N(\omega)$ represents the bose distribution function. The notation $\xi_k^{(\pm;\Omega)}$ is defined as $\xi_k^{(\pm;\Omega)} = \xi_k^{(\pm)} + \Omega$. Substituting Eq. (A2) into Eq. (12) leads to

$$
\begin{aligned}
\frac{I_{(\gamma_2\gamma_2';\gamma_3\gamma_3')}^{(\gamma_1\gamma_1')}}{g^2/2NM\omega} =\ & E_{k-q}^{\gamma_1\gamma_1'(+)} A_{+;k}^{\gamma_2\gamma_2'} A_{+;k}^{\gamma_3\gamma_3'} \cdot \Psi\left(\Xi_k^{(+)}, \Xi_k^{(+)}, \Xi_{k-q}^{(+)} \right) \\
& + E_{k-q}^{\gamma_1\gamma_1'(+)} A_{-;k}^{\gamma_2\gamma_2'} A_{-;k}^{\gamma_3\gamma_3'} \cdot \Psi\left(\Xi_k^{(-)}, \Xi_k^{(-)}, \Xi_{k-q}^{(+)} \right) \\
& + \left(E_{k-q}^{\gamma_1\gamma_1'(+)} A_{+;k}^{\gamma_2\gamma_2'} A_{-;k}^{\gamma_3\gamma_3'} + E_{k-q}^{\gamma_1\gamma_1'(+)} A_{-;k}^{\gamma_2\gamma_2'} A_{+;k}^{\gamma_3\gamma_3'} \right) \cdot \Psi\left(\Xi_k^{(+)}, \Xi_k^{(-)}, \Xi_{k-q}^{(+)} \right) \\
& + E_{k-q}^{\gamma_1\gamma_1'(-)} A_{+;k}^{\gamma_2\gamma_2'} A_{+;k}^{\gamma_3\gamma_3'} \cdot \Psi\left(\Xi_k^{(+)}, \Xi_k^{(+)}, \Xi_{k-q}^{(-)} \right) \\
& + E_{k-q}^{\gamma_1\gamma_1'(-)} A_{-;k}^{\gamma_2\gamma_2'} A_{-;k}^{\gamma_3\gamma_3'} \cdot \Psi\left(\Xi_k^{(-)}, \Xi_k^{(-)}, \Xi_{k-q}^{(-)} \right) \\
& + \left(E_{k-q}^{\gamma_1\gamma_1'(-)} A_{+;k}^{\gamma_2\gamma_2'} A_{-;k}^{\gamma_3\gamma_3'} + E_{k-q}^{\gamma_1\gamma_1'(-)} A_{-;k}^{\gamma_2\gamma_2'} A_{+;k}^{\gamma_3\gamma_3'} \right) \cdot \Psi\left(\Xi_k^{(+)}, \Xi_k^{(-)}, \Xi_{k-q}^{(-)} \right) , \quad \text{(A3)}
\end{aligned}
$$

where we defined

$$E_{k-q}^{\gamma_1\gamma_1'(\pm)} = A_{\pm;k-q}^{\gamma_1\gamma_1'} + A_{\pm;k-q}^{\bar{\gamma}_1\bar{\gamma}_1'} , \quad \text{(A4)}$$

[the first (second) term corresponds to the scattering by u- (v-) phonon, respectively, as in Fig. 2]. Function Ψ is defined as the integral

$$\Psi\left(\xi_k^{(1)}, \xi_k^{(2)}, \xi_{k-q}^{(3)} \right) = \oint_c \frac{dz}{2\pi i} \cdot f(z) \cdot \frac{\sigma_k\left(z, \xi_{k-q}^{(3)} \right)}{\left(z - \xi_k^{(1)} \right)\left(z - \xi_k^{(2)} \right)} , \quad \text{(A5)}$$

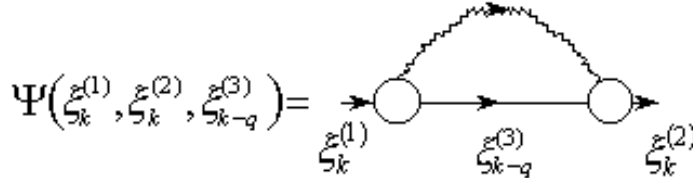corresponding to a diagram shown in Fig. 5.

FIG. 5. Diagram corresponding to $\Psi\left(\xi_k^{(1)}, \xi_k^{(2)}, \xi_{k-q}^{(3)} \right)$

Depending on the degree of the pole, it is evaluated as,

$$\Psi\left(\xi_k^{(1)},\xi_k^{(2)},\xi_{k-q}^{(3)}\right) = f\left(\xi_{k-q}^{(3)}\right)\cdot\left[\frac{f\left(\xi_k^{(1)}\right)}{\left(\xi_k^{(1)}-\xi_{k-q}^{(3;-\omega)}\right)\left(\xi_k^{(1)}-\xi_k^{(2)}\right)}+\frac{f\left(\xi_k^{(2)}\right)}{\left(\xi_k^{(2)}-\xi_k^{(1)}\right)\left(\xi_k^{(2)}-\xi_{k-q}^{(3;-\omega)}\right)}\right.$$
$$\left.+\frac{f\left(\xi_{k-q}^{(3;-\omega)}\right)}{\left(\xi_{k-q}^{(3;-\omega)}-\xi_k^{(1)}\right)\left(\xi_{k-q}^{(3;-\omega)}-\xi_k^{(2)}\right)}\right]$$
$$+\bar{f}\left(\xi_{k-q}^{(3)}\right)\cdot\left[\frac{f\left(\xi_k^{(1)}\right)}{\left(\xi_k^{(1)}-\xi_{k-q}^{(3;+\omega)}\right)\left(\xi_k^{(1)}-\xi_k^{(2)}\right)}+\frac{f\left(\xi_k^{(2)}\right)}{\left(\xi_k^{(2)}-\xi_k^{(1)}\right)\left(\xi_k^{(2)}-\xi_{k-q}^{(3;+\omega)}\right)}\right.$$
$$\left.+\frac{f\left(\xi_{k-q}^{(3;+\omega)}\right)}{\left(\xi_{k-q}^{(3;+\omega)}-\xi_k^{(1)}\right)\left(\xi_{k-q}^{(3;+\omega)}-\xi_k^{(2)}\right)}\right]\,, \tag{A6}$$

for $\xi_k^{(1)}\neq\xi_k^{(2)}$ and

$$\Psi\left(\xi_k,\xi_k,\xi_{k-q}\right) = f\left(\xi_{k-q}\right)\frac{f'\left(\xi_k\right)\left(\xi_k-\xi_{k-q}^{+\omega}\right)-f\left(\xi_k\right)+f\left(\xi_{k-q}^{+\omega}\right)}{\left(\xi_k-\xi_{k-q}^{+\omega}\right)^2}$$
$$+\bar{f}\left(\xi_{k-q}\right)\frac{f'\left(\xi_k\right)\left(\xi_k-\xi_{k-q}^{-\omega}\right)-f\left(\xi_k\right)+f\left(\xi_{k-q}^{-\omega}\right)}{\left(\xi_k-\xi_{k-q}^{-\omega}\right)^2}$$
$$= -f\left(\xi_k\right)\left[f\left(\xi_{k-q}\right)\bar{f}\left(\xi_{k-q}^{-\omega}\right)\cdot P\left[\frac{1}{\left(\xi_k-\xi_{k-q}^{-\omega}\right)^2}\right]\right.$$
$$\left.+\bar{f}\left(\xi_{k-q}\right)\bar{f}\left(\xi_{k-q}^{+\omega}\right)\cdot P\left[\frac{1}{\left(\xi_k-\xi_{k-q}^{+\omega}\right)^2}\right]\right]$$
$$+\bar{f}\left(\xi_k\right)\left[f\left(\xi_{k-q}\right)f\left(\xi_{k-q}^{-\omega}\right)\cdot P\left[\frac{1}{\left(\xi_k-\xi_{k-q}^{-\omega}\right)^2}\right]\right.$$
$$\left.+\bar{f}\left(\xi_{k-q}\right)\left(\xi_{k-q}^{+\omega}\right)\cdot P\left[\frac{1}{\left(\xi_k-\xi_{k-q}^{+\omega}\right)^2}\right]\right]$$
$$\equiv -\left(\Psi_{k,q}^{(1,2)}+\Psi_{k,q}^{(3,4)}\right)\,, \tag{A7}$$

where $\bar{f}\left(\xi_k\right)=1-f\left(\xi_k\right)$. With notations here, the expression for the simple breathing type case with the single band system[42] is expressed as

$$\Delta K^{\text{single}} = \frac{g^2}{4NM\omega}\sum_{kq}\left[-\varepsilon_k\cdot\Psi\left(\xi_k,\xi_k,\xi_{k-q}\right)\right]\,. \tag{A8}$$

19

APPENDIX B: PROPERTY OF THE FUNCTION Ψ IN EQ. (A7)

For the simplest case with single-band electrons and breathing type phonons, Eq. (A8), the filling dependence is determined by $\sum_{kq} [-\varepsilon_k \cdot \Psi (\xi_k, \xi_k, \xi_{k-q})]$. Each term of the function $\Psi (\xi_k, \xi_k, \xi_{k-q})$ in Eq. (A7) contributes when the states $|\xi_k\rangle$, $|\xi_{k-q}\rangle$, and $|\xi_{k-q} \pm \omega\rangle$ are in such configurations as shown in Fig. 6(a).
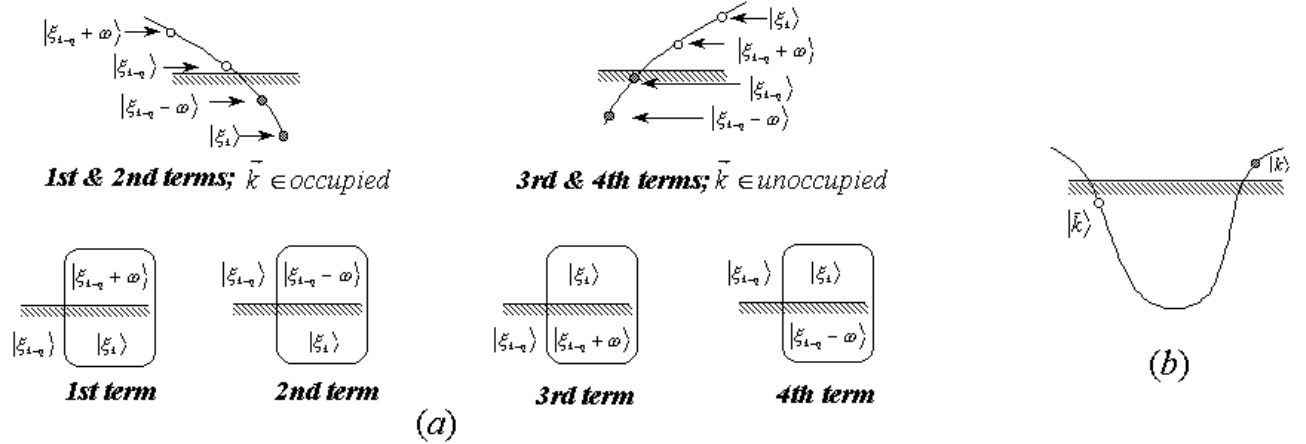

FIG. 6. Configurations of $|\xi_k\rangle$, $|\xi_{k-q}\rangle$, and $|\xi_{k-q} \pm \omega\rangle$ under which each term of Eq. (A7) contributes.

For given and fixed k, the contribution due to each term behaves as shown in Fig. 7 as a function of ξ_{k-q}. Notice that the first and the second terms $(\Psi_{k,q}^{(1,2)})$ are exclusive to the third and fourth terms $(\Psi_{k,q}^{(3,4)})$ each other. Introducing a notation $\bar{k} \equiv k - 2k_F$ [see Fig. 6 (b)], Eq. (A8) is evaluated as,

$$\Delta K^{\text{single}} \sim \sum_{kq} \varepsilon_k \cdot \Psi_{k,q}^{(1,2)} + \sum_{kq} \varepsilon_k \cdot \Psi_{k,q}^{(3,4)} = \sum_{k \in occupied} \left(\varepsilon_k \cdot \sum_q \Psi_{k,q}^{(1,2)} + \varepsilon_{\bar{k}} \cdot \sum_q \Psi_{\bar{k},q}^{(3,4)} \right)$$
$$= \sum_{k \in occupied} \left(\varepsilon_k \cdot S_k^{(1,2)} + \varepsilon_{\bar{k}} \cdot S_{\bar{k}}^{(3,4)} \right) , \tag{B1}$$

where $S_k^{(1,2)} > 0$ and $S_k^{(3,4)} < 0$ are the quadratures of the shaded areas with signs depicted in Fig. 7 (a) and (b), respectively.
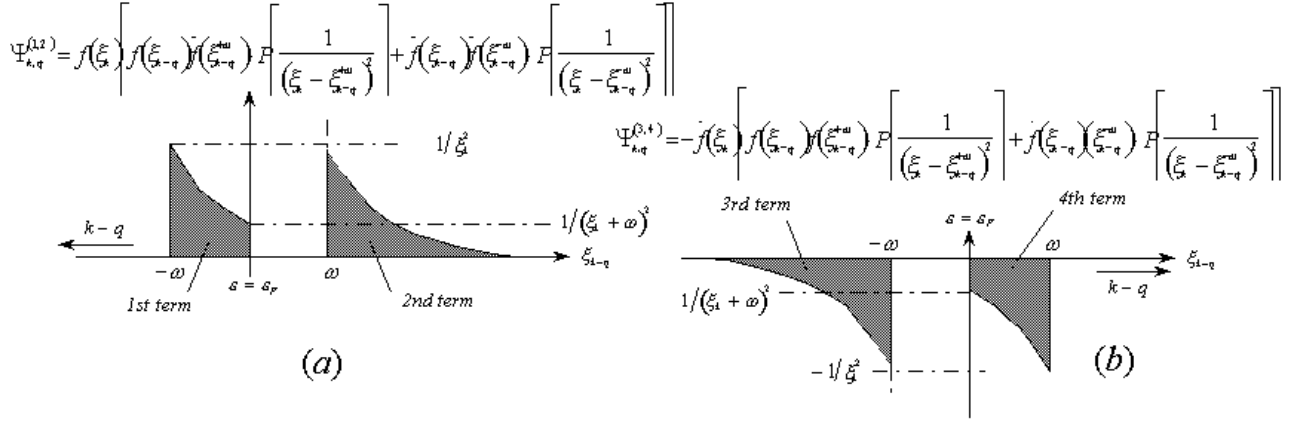
FIG. 7. Behavior of each contribution of terms in Eq. (A7) as a function of ξ_{k-q} for fixed k.

It can be written as $S_{\bar{k}}^{(3,4)} = -S_k^{(1,2)} + \delta S_k$ with a small deviation δS_k which reflects the difference between the band curvature at $|k\rangle$ and $|\bar{k}\rangle$ shown in Fig. 6 (b). δS_k vanishes when the system is half-filled where the fermi level locates at the middle of the band. Equation (B1) is then evaluated as,

$$\Delta K^{single} \sim \sum_{k \in occupied} \left[(\mu + \xi_k) S_k^{(1,2)} + (\mu - \xi_k) \left(-S_k^{(1,2)} + \delta S_k \right) \right] = 2 \sum_{k \in occupied} \xi_k S_k^{(1,2)} + \delta K \ , \quad (B2)$$

with a small δK compared with the first term. Because $\xi_k \leq 0$ for occupied states the result has therefore definite sign. From Fig. 7, it is understood that the contributions mainly come from the vicinity of the fermi level. It thus means that the result scales to the density of states at the fermi level.

REFERENCES

[1] K. Chahara, T. Ohono, M. Kasai, Y. Kanke, and Y. Kozono, Appl. Phys. Lett. **62**, 780 (1993).

[2] R. von Helmolt, J. Wecker, B. Holzapfel, L. Schultz, and K. Samwer, Phys. Rev. Lett. **71**, 2331 (1993).

[3] Y. Tokura, A. Urushibara, Y. Moritomo, T. Arima, A. Asamitsu, G. Kido, and N. Furukawa, J. Phys. Soc. Jpn. **63**, 3931 (1994); A. Urushibara, Y. Moritomo, T. Arima, A. Asamitsu, G. Kido, and Y. Tokura, Phys. Rev. B **51**, 14 103 (1995).

[4] S. Jin, T. H. Tiefel, M. McCormack, R. A. Fastnacht, R. Ramesh, and L. H. Chen, Science **264**, 413 (1994).

[5] C. Zener, Phys. Rev. **82**, 403 (1951).

[6] P. W. Anderson and H. Hasegawa, Phys. Rev. **100**, 675 (1955).

[7] P. G. de Gennes, Phys. Rev. **118**, 141 (1960).

[8] S. Ishihara, M. Yamanaka, and N. Nagaosa, Phys. Rev. B **56**, 686 (1997).

[9] N.Nagaosa, S.Murakami, and H.C.Lee, Phys. Rev. B **57**, R6767 (1998).

[10] R. Killian and G. Khaliullin, Phys. Rev. B **58**, R11 841 (1998).

[11] Y. Endoh, K. Hirota, S. Ishihara, S. Okamoto, Y. Murakami, A. Nishizawa, T. Fukuda, H. Kimura, H. Nojiri, K. Kaneko, and S. Maekawa, Phys. Rev. Lett. **82**, 4328 (1999).

[12] G. Khaliullin and R. Kilian, Phys. Rev. B **61**, 3494 (2000).

[13] A. Takahashi and H. Shiba, J. Phys. Soc. Jpn. **69**, 3328 (2000).

[14] R. Maezono and N. Nagaosa, Phys. Rev. B **62**, 11576 (2000).

[15] J. Brink and D. Khomskii, Phys. Rev. B **63**, 140416 (2001).

[16] A.J. Millis, P.B. Littlewood and B.I. Shrainman, Phys. Rev. Lett. **74**, 5144 (1995).

[17] A.J. Millis, B.I. Shrainman and R. Mueller, Phys. Rev. Lett. **77**, 175 (1996).

[18] A.J. Millis, R. Mueller and B.I. Shraiman, Phys. Rev. B **54**, 5389 (1996). *ibid.* **54**, 5405 (1996).

[19] A.J. Millis, Phys. Rev. B **53**, 8434 (1996).

[20] H. Röder, J. Zang, and A.R. Bishop, Phys. Rev. Lett. **76**, 1356 (1996).

[21] R. Kajimoto, H. Yoshizawa, H. Kawano, H. Kuwahara, Y. Tokura, K. Ohoyama and M. Ohashi, Phys. Rev. B **60**, 9506 (1999).

[22] Y. Moritomo, T. Akimoto, A. Nakamura, K. Ohoyama, and M. Ohashi, Phys. Rev. B **58**, 5544 (1998).

[23] Y. Tokura, and N. Nagaosa, Science **288**, 462 (2000).

[24] T. Akimoto, Y. Moritomo, K. Ohoyama, S. Okamoto, S. Ishihara, S. Maekawa, and A. Nakamura,, Phys. Rev. B **59**, R14153 (1999)

[25] M. Kubota, H. Fujioka, K. Hirota, K. Ohoyama, Y. Moritomo, H. Yoshizawa, and Y. Endoh, J. Phys. Soc. Jpn. **69**, 1606 (2000).

[26] C.D. Ling, J.E. Millburn, J.F. Mitchell, D.N. Argyriou, J. Linton, H. Bordallo, Phys. Rev. B **62**, 15096 (2000).

[27] R. Maezono, S. Ishihara and N. Nagaosa, Phys. Rev. B **57**, R13 993 (1998), *ibid.* **58**, 11 583 (1998).

[28] R. Maezono, and N. Nagaosa, Phys. Rev. B **61**, 1825 (2000).

[29] J. Brink, and D. Khomskii, Phys. Rev. Lett. **82**, 1016 (1999).

[30] L. Sheng, C.S. Ting, Phys. Rev. B **60**, 14809 (1999).

[31] S. Okamoto, S. Ishihara, and S. Maekawa, Phys. Rev. B **61**, 451 (2000).

[32] S. Okamoto, S. Ishihara, and S. Maekawa, Phys. Rev. B **61**, 14647 (2000).

[33] Z. Fang, I.V. Solovyev, and K. Terakura, Phys. Rev. Lett. **84**, 3169 (2000).

[34] S. Okamoto, S. Ishihara, and S. Maekawa, Phys. Rev. B **61**, 451 (2000).

[35] P. Benedetti and R. Zeyher, Phys. Rev. B **58**, 14 320 (1998).

[36] A. Georges, G. Kotliar, W. Krauth, and M.J. Rozenberg, Rev. of Mod. Phys. **68**, 13 (1996).

[37] R. Maezono and N. Nagaosa, Phys. Rev. B **61**, 1189 (2000).

[38] M. Quijada, J. Cerne, J.R. Simpson, H.D. Drew, K.H. Ahn, A.J. Millis, R. Shreekala, R. Ramesh, M.Rajeswari, and T. Venkatesan, Phys. Rev. B **58**, 16 093 (1998).

[39] G. D. Mahan, in *Many-Particle Physics, 2nd ed.* (Plenum Press, New York,1990) Chap. 4.

[40] Z. X. Shen, A. Lanzara, S. Ishihara, and N. Nagaosa, cond-mat/0108381 and references therein.

[41] K. Yamamoto, T. Kimura, T. Ishikawa, T. Katsufuji, and Y. Tokura, Phys. Rev. B **61**, 14 706 (2000).

[42] D. J. Kim, in *New Perspectives in Magnetism of Metals.* (Kluwer Academic/Plenum Publishers, New York,1999) Chap. 9.

[43] K. I. Kugel and D. I. Khomskii, Pis'ma Zh. Éksp. Teor. Fiz. **15**, 629 (1972) [JETP Lett. **15**, 446 (1972)]; D. I. Khomskii and K. I. Kugel, Solid State Commun. **13**, 763 (1973).

[44] J. Kanamori, J. Appl. Phys. **31**, 14S (1960).

[45] K. Yamamoto, T. Kimura, T. Ishikawa, T. Katsufuji, and Y. Tokura, Phys. Rev. B **61**, 14 706 (2000).